Nonlinear Interaction between Neighboring Data Channels and a Frequency Signal in a Commercial Optical Fiber Communication System

by

Patrick Sykes

Table of Contents

Chapter 1: Introduction

Improvements in optical frequency references allow them to be a better reference than current atomic clock standards. This opens up the potential to improve precision and accuracy in timekeeping systems as well as a redefinition of the second. That increase in precision and accuracy are limited by the synchronisation between those clocks using optical standards. There is some frequency uncertainty in a reference which becomes exacerbated as the reference is transmitted through a medium and influenced by the environment. Understanding the mechanisms for frequency distortion and controlling them where possible give stricter bounds on the frequency error.

Accurate timekeeping is required in the Global Positioning System (GPS) satellites and receivers, transaction logging, and research experiments. Currently, there are techniques and systems for time and frequency transfer in wireless communication systems. A common method is the two-way satellite time and frequency transfer system which enables two laboratories to use a satellite as a common link to synchronize their clocks. These wireless systems are typically accurate to within $1 - 10$ ns [1]. Beyond improving the time accuracy, there is a significant issue of inaccessibility with satellite

systems, which makes hardware maintenance and upgrades difficult and the satellites themselves vulnerable to attack. Fiber optics can become a substitute for transfer, especially if one can take advantage of the existing fiber telecommunications infrastructure.

Research networks are increasingly transmitting time and frequency signals along with data over fiber optic communication systems. These networks include Réseau Fibré Métrologique à Vocation Européenne (REFIMEVE+) in France [2], PIONIER in Poland [3], and the White Rabbit networks used for CERN accelerator sites and GSI's Facility for Antiproton and Ion Research [4]. A larger European optical time and frequency distribution network called CLONETS is planned [5]. The REFIMEVE+ project has demonstrated frequency transfer over optical fiber with a stability of 10^{-16} at 1 s and 10^{-19} at 10^4 s over a distance of 1480 km [2]. These systems place the frequency signal on a center frequency assigned for data transmissions.

Many impairments are introduced to the signal from the fiber [6]. In a typical optical communication system, there are many data channels centered at different optical wavelengths which is a technique called wavelength division multiplexing (WDM). Each channel has some finite bandwidth so that they do not overlap in the frequency domain. In this thesis, we will be considering the possibility of transmitting a frequency signal in the interstices of the WDM channels. We will examine the limits that fiber impairments impose on this frequency signal in a long-haul system. Signal impairments include amplified spontaneous emission (ASE) noise from amplifiers, disper-

sion, and the Kerr nonlinearity, scattering nonlinearities, Rayleigh, Brillouin, and Raman scattering, can also impair the signal [6] [7]. Preliminary work indicates that this frequency signal can be transmitted with both a narrow bandwidth (< 100 MHz) and low power ($< 10\ \mu W$) when compared to a data channel. The bandwidth of a data channel in a long-haul system is typically $10 - 100$ GHz [8], while a typical power in a terrestrial long-haul system is 0 dBm or 1 mW at the transmitter and less than -10 dBm or 0.1 mW prior to an amplifier as the signal attenuates. In this case, the most important impairment that the frequency signal suffers is due to cross-phase modulation between the frequency signal and the neighboring data channels. In this thesis, we will quantify the impact of cross-phase modulation on the frequency signal and determine the limits that it imposes.

The individual data channels are modulated to transmit information. Modulation formats are on-off keying (OOK), binary phase shift keying (BPSK), quadrature phase shift keying (QPSK), and differential phase shift keying (DPSK) [6]. An OOK signal is the simplest example, a binary 0 is represented as the absence of power and a binary 1 is some non-zero power above a threshold to distinguish a signal from noise. There cannot be a sharp transition from a 0 to a 1 and vice versa, because a communication channel can only occupy a limited bandwidth. In practice, each bit occupies a window of time where its value is held for a short time. The signal can start building up to a 1 in its preceding bit window and decay back to a 0 in its following bit window. The bits overlap into their neighboring windows and

the amount of overlap is characterized by a roll-off parameter. This overlap is known as intersymbol interference [9].

The frequency signal will have periodic zero crossings. However, nonlinearities from the fiber may alter the timing of the zero crossings. This phase change causes the frequency signal to appear as if it were different frequencies. We must find the distribution of the amplitude of the data channel in order to calculate its variance and its impact on the phase change of the frequency signal. The distribution of the amplitude of the channel is mainly influenced by dispersion. We calculate the effect of dispersion on an OOK signal after the signal has propagated a distance long enough for dispersion to completely spread it out.

Chapter 2 introduces methods for measuring frequency stability of oscillators. We present the reasoning behind formulating different time stability measures, and the failures of usual statistical measures (mean, variance, etc.). Then we reveal the relations between each of the methods. We give a recommendation of the second structure function and Allan deviation for the measures of phase and frequency stability, respectively.

Chapter 3 is an overview of the common impairments a signal experiences in an optical fiber. The impairments will affect both a data channel and the frequency signal. Here the limits of the impairments will be investigated which will inform power and frequency requirements on the frequency signal. After eliminating the negligible impairments, we highlight cross-talk as the principal cause of phase distortion in the frequency channel.

Chapter 4 contains the results of the phase noise computations. We perform statistical and time stability analysis on the phase noise to determine the amount of frequency fluctuation on the frequency signal.

Chapter 5 concludes the thesis.

Chapter 2: Phase and Frequency Stability Measures

2.1 Introduction

Keeping time requires a periodic event that can be counted and a time reference point. To synchronize two clocks: they need to phase match the periodic event, and transfer the reference point. Figuring out the reference point requires calculating an approximate delay due to propagation which can be achieved by transmitting a time point and then wait to receive confirmation from the other system. The White Rabbit Project achieves synchronization by using Synchronous Ethernet for syntonization, and IEEE 1588 Precision Time Protocol [4] to determine the initial time point.

However, no frequency source is perfect, there can be initialization errors, manufacturing flaws, and environmental influences. The various environmental causes for oscillator instability are pressure, temperature, magnetic fields. There are excellent references on the history of clocks and oscillator errors [10] [11]. This thesis investigates the instabilities caused by optical impairments from the fiber medium and amplifiers, environmental effects or issues inherent to the oscillator source and setup are covered in other stud-

ies [12] [13] [14].

A frequency source can be represented as

$$u_c(t) = (U_0 + \epsilon(t)) \sin(\omega_0 t + \phi(t)) \tag{2.1}$$

The U_0 is the amplitude and $\epsilon(t)$ is amplitude fluctuation. The quantities ω_0 is the nominal angular frequency and $\phi(t)$ is the phase fluctuation. The amplitude fluctuation must be much less than the nominal amplitude, $|\epsilon(t)| << |U_0|$, otherwise eq. 2.1 is an amplitude modulated signal and outside the scope of this work. Similarly, in order to avoid frequency modulation the condition $|\dot{\phi}(t)| << |\omega_0|$ is necessary, where the dot represents the time derivative.

The instantaneous frequency is defined as the time derivative of the total phase

$$\omega(t) = \frac{d}{dt}\left[\omega_0 t + \phi(t)\right] = \omega_0 + \dot{\phi}(t). \tag{2.2}$$

Most literature uses the fractional frequency, $y(t)$, and the phase time, $x(t)$,

$$y(t) = \frac{\omega(t) - \omega_0}{\omega_0} = \frac{\dot{\phi}(t)}{\omega_0}, \qquad x(t) = \int_0^t y(\tau) d\tau = \frac{\phi(t)}{\omega_0} \tag{2.3}$$

but we will mainly work with the ϕ and $\dot{\phi}$ quantities. The relations to y and x are shown above in eq. 2.3. Using ϕ and $\dot{\phi}$ emphasizes the phase and frequency error of the signal and is more convenient in theoretical work, whereas the fractional frequency and phase time are better suited for physical

measurements. Note also that x and ϕ are measured instantaneously, while measuring y requires a time average

$$\bar{y}_k = \frac{1}{\tau} \int_{t_k}^{t_k+\tau} y(t)dt. \tag{2.4}$$

The invention of atomic clocks necessitated a means of quantifying frequency stability [15] [16]. Since the errors have a random component, the use of statistics like the power spectral density (PSD) is a fundamental measure. Calculating a true variance of the process may not be realizable leading to the invention of the Allan variance. There is third method using structure functions. In this chapter, we will describe these different measures and then show the relationships between them.

2.2 Power Spectral Density

The power spectral density of the phase noise can be obtained by feeding the output of a phase demodulator through a spectrum analyser, and, similarly, the PSD of the frequency noise by using a spectrum analyser on the output of a frequency demodulator.

For any of the x, y, ϕ, and $\dot{\phi}$ the autocorrelation is defined as

$$R_\phi(\tau) = E\{\phi(t)\phi(t+\tau)\} = \lim_{T\to\infty} \frac{1}{T} \int_0^T \phi(t)\phi(t+\tau)dt. \tag{2.5}$$

And the PSD is the Fourier transform of the autocorrelation

$$S_\phi(\omega) = 2\int_0^\infty R_\phi(\tau)\cos(\omega\tau)d\tau \tag{2.6}$$

$$R_\phi(\tau) = \frac{1}{\pi}\int_0^\infty S_\phi(\omega)\cos(\omega\tau)d\omega \tag{2.7}$$

Evaluating $R_\phi(\tau)$ at $\tau = 0$ gives us the second moment of ϕ,

$$R_\phi(0) = E\{[\phi(t)]^2\} = \int_0^\infty S_\phi(\omega)d\omega.$$

This can be considered the total "power" of the signal. If we compare the power spectrum of two different sources, then the one with lower total power will typically have less error.

The power spectrum densities for each of our quantities have the relations:

$$S_{\dot\phi}(\omega) = \omega^2 S_\phi(\omega) \tag{2.8}$$

$$S_y(\omega) = \frac{\omega^2}{\omega_0^2}S_\phi(\omega) \tag{2.9}$$

$$S_x(\omega) = \frac{1}{\omega_0^2}S_\phi(\omega) \tag{2.10}$$

Oscillator noise can typically be decomposed into a power series $S_\phi(\omega) = \sum_{k=0}^{4} h_k\omega^{-k}$ [17]. The ω^0 term is considered white ϕ noise, the ω^{-1} term is considered flicker ϕ noise, and ω^{-2} to be random walk ϕ noise. Since $S_{\dot\phi}(\omega) = \omega^2 S_\phi(\omega)$, the powers in the series increase by 2 and we see that the ω^{-3} term is flicker $\dot\phi$ and ω^{-4} is random walk $\dot\phi$. When plotting the power spectral

density of oscillator noises on a log-log plot, the various regions where white, flicker, and random walk dominate are indicated by slopes corresponding to the powers in the power series.

The techniques in Blackman-Tukey can be used to estimate the power spectral density when dealing with finite samples [18].

2.3 Allan Variance

The distribution of frequency error is difficult to determine because the error is typically nonstationary. The sample variance from finitely many measurements may not converge to the true variance of the process as the number of samples goes to infinity. The Allan Variance is the mean of sample variances calculated over an interval. The definition is based on the fractional frequency y and phase time x, however we will convert it into phase ϕ terms. We use the averaged quantity $\bar{y}_k$ defined in eq. 2.4.

The N sample mean is defined as

$$\mu = \frac{1}{N}\sum_{k=1}^{N} \bar{y}_k. \tag{2.11}$$

The sample mean can then be used for the N sample variance

$$\sigma_S^2(N) = \frac{1}{N-1}\sum_{k=1}^{N} \left(\bar{y}_k - \mu\right)^2 = \frac{1}{N-1}\sum_{k=1}^{N} \left(\bar{y}_k - \frac{1}{N}\sum_{i=1}^{N} \bar{y}_i\right)^2. \tag{2.12}$$

The Allan variance [15] is the mean of the sample variances over all time.

$$\sigma_A^2(N,\tau) = \langle \sigma_S^2(N) \rangle = \left\langle \frac{1}{N-1} \sum_{k=1}^{N} \left(\bar{y}_k - \frac{1}{N} \sum_{i=1}^{N} \bar{y}_i \right)^2 \right\rangle \tag{2.13}$$

The original Allan variance utilises N samples, but typically the two-sample Allan variance is used, $N = 2$,

$$\sigma_A^2(2,\tau) = \frac{1}{2} \langle [\bar{y}_{k+1} - \bar{y}_k]^2 \rangle. \tag{2.14}$$

It is impractical to test over all time so one can compute the Allan variance from a set of M samples,

$$\sigma_A^2(\tau, M) = \frac{1}{2(M-1)} \sum_{k=1}^{M-1} \left(\bar{y}_{k+1} - \bar{y}_k \right)^2 \tag{2.15}$$

The averaged fractional frequency has the relation $\bar{y}_k = [\phi(t_k+\tau) - \phi(t_k)]/(\omega_0 \tau)$. Thus, the Allan variance is then re-written in terms of the phase,

$$\sigma_A^2(\tau) = \frac{1}{2} \left\langle \left[\frac{\phi(t_k + 2\tau) - \phi(t_k + \tau)}{\omega_0 \tau} - \frac{\phi(t_k + \tau) - \phi(t_k)}{\omega_0 \tau} \right]^2 \right\rangle. \tag{2.16}$$

2.4 Structure Functions

The structure functions are based off of studies that Kolmogorov performed on turbulence [19]. The oscillator phase $\phi(t)$ can be modeled as the process,

$$\phi(t) = \omega_0 t + \sum_{k=2}^{N} \frac{\Omega_{k-1}}{k!} t^k + \psi(t) + \phi_0. \tag{2.17}$$

The summation in eq. 2.17 is the long term phase drift. This long term drift is the source of nonstationarity. The process $\psi(t)$ is the short term phase instability and can be considered stationary. The structure functions can be used to eliminate the long term drift.

The first difference equation

$$\Delta\phi(\tau) := \Delta\phi(t;\tau) = \phi(t+\tau) - \phi(t) \tag{2.18}$$

is the total phase accumulated over the interval τ. The N-th difference equation is defined recursively

$$\Delta^N\phi(\tau) = \Delta^{N-1}\left[\Delta\phi(\tau)\right]. \tag{2.19}$$

Whenever the process $\phi(t)$ is a (wide-sense) stationary process, the mean of the N-difference equation is 0. The N-th structure function is then the second moment of the N-th difference equation

$$D_\phi^{(N)}(\tau) = \langle(\Delta^N\phi(\tau))^2\rangle. \tag{2.20}$$

Since the first difference equation is the total phase accumulation, $\sqrt{D_{\phi}^{(1)}(\tau)}$ is the mean phase accumulation. Dividing the first difference equation by the time difference τ is equivalent to discrete differentiation in time, so $[\phi(t+\tau)-\phi(t)]/\tau$ is considered the frequency accumulation over τ, and the standard deviation of this term is the mean frequency accumulation [19].

The random process doesn't necessarily require (wide-sense) stationarity but the difference equation can be stationary. For example, if the process is an n-th order polynomial with an additive stationary process term, then the M-th difference equation eliminates all the polynomial terms whenever $M > n$ and we are left with the M-th difference of the stationary process.

The structure functions can be computed to higher accuracy using less data than the correlation function [20]. This is particularly noticeable for "flicker" noises that has frequency characteristics ω^{-1} and is common in oscillator noise.

2.5 Converting between different measures

The power spectral density can be considered the most fundamental measurement of frequency stability. However, sampling the time data points presents issues for calculating an accurate power spectrum. Most importantly, there may not be enough frequency resolution for low frequency deviations with high power, ω^{-1}, referred to as "flicker noise". When the power spectrum is available then it can be converted to the structure functions and the Al-

lan variance. The reverse is not generally true, though sometimes possible through the use of difficult Mellin transformations [21] [19].

Allan variance to structure function

We now show that the Allan variance is proportional to a certain structure function. Use the Allan variance definition in eq. 2.16, then

$$\sigma_A^2(2,\tau) = \frac{1}{2}\left\langle \left[\frac{\phi(t_k+2\tau)-\phi(t_k+\tau)}{\omega_0\tau} - \frac{\phi(t_k+\tau)-\phi(t_k)}{\omega_0\tau} \right]^2 \right\rangle \tag{2.21}$$

$$= \frac{1}{2\omega_0^2\tau^2}\langle [\phi(t_k+2\tau) - 2\phi(t_k+\tau) + \phi(t_k)]^2 \rangle. \tag{2.22}$$

The t_k are arbitrary when averaging over all time, so the averaging term is the form of the structure function $D_\phi^{(2)}(\tau)$. Apart from the extra division by $2\omega_0^2$, we can interpret the Allan variance as the approximate short term average frequency accumulation over τ.

Power spectral density to structure function

The relation between the power spectral density and the structure function depends on the long term frequency drift of the oscillator and whether the M-th difference equation is stationary [19]. Suppose that the drift is compensated or $M > N$, where N is the highest order polynomial term for the drift, then

$$D_\phi^{(M)}(\tau) = 2^{2M}\int_{-\infty}^{\infty} \sin^{2M}\left(\frac{\omega\tau}{2}\right) S_\phi(\omega)d\omega. \tag{2.23}$$

Power spectral density to Allan variance

Since we demonstrated that the Allan variance is proportional to a structure function in eq. 2.21, we combine the results from the last two sections,

$$\sigma_A^2(2,\tau) = \frac{2^2}{\omega_0^2\tau^2}\int_{-\infty}^{\infty} \sin^4\left(\frac{\omega\tau}{2}\right) S_\phi(\omega)d\omega. \tag{2.24}$$

2.6 Chapter remarks

We will be using the structure functions, specifically $D_\phi^{(1)}(\tau)$, as our preferred measure of stability. The reason for this is that it requires fewer samples than the correlation to compute "flicker" noise and it is simple to implement and interpret. The Allan Deviation will also be sparingly because it is a common measure of stability in oscillator communities and we have reinterpreted it as proportional to a specific structure function $D_\phi^{(2)}(\tau)$. The power spectral density is preferred for experimental measurements.

Chapter 3: Optical Fiber Impairments

3.1 Introduction

Propagation through optical fiber creates distortion for a frequency signal. Previous work highlights the various optical impairments in fiber and their influence on a frequency signal [22], in this chapter we briefly summarize that work and relate it to our simulations.

The propagation of light through optical fiber is modeled by the Nonlinear Schrödinger (NLS) Equation [7],

$$\frac{\partial u}{\partial z} + \beta_1 \frac{\partial u}{\partial t} + \frac{i\beta_2}{2}\frac{\partial^2 u}{\partial t^2} + \frac{\alpha}{2}u = i\gamma|u|^2 u. \tag{3.1}$$

where u is the pulse envelope, β_1 is the group velocity, β_2 is the group velocity dispersion, α is the attenuation, and γ is the Kerr nonlinearity.

We split the input signal into a combination of two signals, u_d the data channel and u_f the frequency channel. It is helpful to define a reference frame moving with the frequency signal $T = t - z/v_f$, where T is the retarded time and v_f is the group velocity of the frequency signal. The data channel now travels at the group-velocity difference $d = (v_f - v_d)/(v_f v_d)$.

The right hand side of eq. 3.1 is nonlinear, so the sum of two signals must be handled carefully,

$$|u_d + u_f|^2(u_d + u_f) = (u_d + u_f)(u_d^* + u_f^*)(u_d + u_f)$$
$$= |u_d|^2 u_d + 2|u_f|^2 u_d + u_f^2 u_d^* + u_d^2 u_f^* + 2|u_d|^2 u_f + |u_f|^2 u_f. \quad (3.2)$$

We can now break eq. 3.1 into two differential equations,

$$\frac{\partial u_f}{\partial z} + \frac{\alpha_f}{2} u_f + \frac{i\beta_{2f}}{2}\frac{\partial^2 u_f}{\partial T^2} = i\gamma_f \left(|u_f|^2 u_f + 2|u_d|^2 u_f + u_d^2 u_f^*\right) \quad (3.3)$$

$$\frac{\partial u_d}{\partial z} + \frac{\alpha_d}{2} u_d + d\frac{\partial u_d}{\partial T} + \frac{i\beta_{2d}}{2}\frac{\partial^2 u_d}{\partial T^2} = i\gamma_d \left(|u_d|^2 u_d + 2|u_f|^2 u_d + u_f^2 u_d^*\right). \quad (3.4)$$

The subscripts d and f correspond to the material properties α, β_2, and γ for data and frequency channels, respectively. The term $d\partial u_d/\partial T$ in eq. 3.4 governs the group velocity of the data channel relative to the reference frame following the frequency signal.

In this chapter we will define each of the impairment terms in eqs. 3.3 and 3.4 and give suitable conditions under which they will negligibly affect the phase stability. Then we will further examine the primary source of phase instability.

3.2 Optical Impairments

In the previous section, we highlighted the nonlinear term and how the sum of two signals creates multiple nonlinear terms. In this section, we shall examine each of the terms related to an optical impairment and how that impairment

affects the frequency signal. In the analysis we introduce conditions on the data and frequency channel to make terms in the decoupled equations 3.3 and 3.4 negligible.

3.2.1 Attenuation and Amplified Spontaneous Emission (ASE)

Attenuation appears in the decoupled equations above as

$$\frac{\partial u_f}{\partial z} = -\frac{\alpha_f}{2} u_f, \qquad \frac{\partial u_d}{\partial z} = -\frac{\alpha_d}{2} u_d.$$

The attenuation is due to absorption and scattering and will decrease the optical power of the frequency signal exponentially. Amplifiers are spaced periodically to compensate for the loss of optical power, but they add noise due to spontaneous emission of photons in the process. The ASE is a white noise source with noise power [6]

$$\sigma^2_{ASE} = n_{sp} h \nu_0 (G-1) \Delta\nu \tag{3.5}$$

where n_{sp} is called the spontaneous emission factor, h is Planck's constant, ν_0 is the center frequency, G is the gain of the amplifier, and $\Delta\nu$ is the bandwidth of the signal. The bandwidth of the frequency signal will be very narrow making the ASE noise negligible. Notice that the equations 3.3 and 3.4 are dependent on the frequency signal power, we want to keep this dependency small but so small such that the signal is dominated by ASE noise.

Consider an optical communication system that has 800 km distance and 80 km amplifier separation operating at the wavelength 1.5 μm with loss $\alpha_{dB} = 0.2$ dB/km. This implies a gain $G = 40$. A typically amplifier will have noise figure $n_{sp} = 2$ with 10 amplifiers altogether. Supposing the narrow bandwidth of the frequency signal is on the order of 10 MHz, then the total noise power is 1 nW.

3.2.2 Chromatic Dispersion

The dispersion appears as

$$\frac{\partial u_f}{\partial z} = -\frac{i\beta_{2f}}{2}\frac{\partial^2 u_f}{\partial T^2}, \qquad \frac{\partial u_d}{\partial z} = -\frac{i\beta_{2d}}{2}\frac{\partial^2 u_d}{\partial T^2}.$$

This impairment is pulse spreading because the various frequency components of a channel travel at different velocities. The time spread due to dispersion is [6]

$$\tau_{disp} = DL\Delta\lambda \tag{3.6}$$

where D is the dispersion parameter, L is the length of the fiber, and $\Delta\lambda$ is the range of wavelengths. Since $\Delta\lambda = \lambda\Delta\nu/\nu$, we see that the narrow bandwidth of the frequency signal will cause a negigible spread in time.

For the optical communication system in the previous example and the frequency signal centered at a wavelength $\lambda \approx 1.5$ μm, we find $\tau_{disp} = 1$ ps.

3.2.3 Self-Phase Modulation (SPM)

The terms

$$\frac{\partial u_f}{\partial z} = i\gamma_f |u_f|^2 u_f, \qquad \frac{\partial u_d}{\partial z} = i\gamma_d |u_d|^2 u_d$$

correspond to self-phase modulation. This distortion takes the form of a phase shift dependent on the signal power. Thus, linear attenuation limits the effect over some length after each amplifier. The effective length is $L_{eff} = (1/\alpha)[1 - \exp(-\alpha L)]$, so $L_{eff} \approx 20$ km for $\alpha_{dB} = 0.2$ dB/km.

The maximum phase shift due to self-phase modulation for a length of fiber between amplifiers is [7]

$$\phi_{SPM} = \gamma P_f L_{eff} \tag{3.7}$$

where P_f is the power of the frequency signal. The total maximum phase shift will be a multiplication of eq. 3.7 by the number of amplifiers in the fiber link.

For our typical system, $\gamma = 1.3$ W^{-1}km^{-1}, $L_{eff} = 20$ km, and giving an upperbound on ϕ_{SPM} of 1 radian, then the upper bound on the frequency signal power is 3.8 mW.

3.2.4 Four-Wave Mixing (FWM)

The terms

$$\frac{\partial u_f}{\partial z} = i\gamma_f u_d^2 u_f^*, \qquad \frac{\partial u_d}{\partial z} = i\gamma_d u_f^2 u_d^*$$

correspond to four-wave mixing. For any two data signals centered at ω_1 and ω_2 with corresponding wavenumbers $\beta(\omega_1)$ and $\beta(\omega_2)$, then FWM creates a parasitic wave whenever $\omega_1 + \omega_2 = 2\omega_f$ and $\beta(\omega_1) + \beta(\omega_2) = 2\beta(\omega_f)$. This phase-matching condition is avoidable as long as the channels are located away from the zero dispersion wavelength of the fiber. Placing the frequency signal greater than 5 times its bandwidth away from the zero dispersion wavelength should eliminate this impairment.

3.2.5 Cross-Phase Modulation (XPM)

The remaining terms,

$$\frac{\partial u_f}{\partial z} = i2\gamma_f |u_d|^2 u_f, \qquad \frac{\partial u_d}{\partial z} = i2\gamma_d |u_f|^2 u_d$$

correspond to cross-phase modulation. XPM represents the cross-talk between two channels. This error becomes negligible when the group velocity difference between the data and frequency channels is large. This typically occurs when the two channels are spaced very far apart in the frequency spectrum. Therefore, the effects of XPM on the frequency signal only needs to be computed for the two nearest neighboring data channels. Since our goal is to place the frequency signal on the interstices of two data channels, XPM will become our primary source of frequency distortion. The limitation on the optical power of the frequency signal for the other effects, will eliminate the effect of XPM on the data channels from the frequency channel.

3.3 Phase noise on the frequency signal

Applying limits on the system parameters, then the uncoupled equations 3.3 and 3.4 simplify to the following equations

$$\frac{\partial u_f}{\partial z} = i2\gamma_f |u_d|^2 u_f \tag{3.8}$$

$$\frac{\partial u_d}{\partial z} + \frac{\alpha_d}{2} u_d + d\frac{\partial u_d}{\partial T} + \frac{i\beta_{2d}}{2}\frac{\partial^2 u_d}{\partial T^2} = i\gamma_d |u_d|^2 u_d. \tag{3.9}$$

Suppose the frequency signal is of the form $u_f(z,T) = u_f(0,T)\exp(i\phi(z,T))$, where $u_f(0,T)$ is the initial frequency source and $\phi(z,T)$ is phase distortion due to XPM. Then, we can solve for the phase distortion using 3.8,

$$\phi(z,T) = 4\gamma_f \int_0^z |u_d(0, T-\zeta d)|^2 d\zeta. \tag{3.10}$$

The frequency signal will be equally spaced between two neighboring data channels so eq. 3.10 was doubled.

The data channel is now subject to the effects of loss, dispersion, time shift due to group velocity differences, and self-phase modulation. Now studying the phase distortion on the frequency signal depends entirely on the evolution of the data channel as it propagates through the fiber.

3.4 Chapter Remarks

By limiting the frequency signal's optical power and its location on the frequency spectrum, we can limit the causes of phase distortion due to various optical impairments. This leaves the distortion to one principal source, XPM. In the next chapter, we perform computations to estimate $\phi(z, T)$ using common system parameters of a commercial fiber optic communication system.

Chapter 4: Results

4.1 Introduction

In the previous section, we presented limitations on the parameters of a commercial optical communication system that would limit the distortion on a frequency signal located on the interstices of two data channels in a DWDM scheme. The result was a phase distortion due to cross-talk (XPM) in the form

$$\phi(z,T) = 4\gamma \int_0^z |u_d(0, T - d\zeta)|^2 d\zeta. \tag{4.1}$$

This shows that the phase distortion is dependent on the length of fiber, the relative velocity difference between the frequency signal and the data channels, and the power of the data channel while it changes over the course of its propagation. We can now vary these parameters and investigate their affect on the frequency stability of the frequency signal.

We choose values for the data channel power and Kerr nonlinearity γ that resemble commercial optical communication systems, these values are used in those systems to avoid nonlinear distortions. This removes the nonlinear

term in eq. 3.9 and the data channel can be solved in the Fourier domain,

$$u_d(0, T - zd) = \mathcal{F}^{-1}\left\{U_d(0,\omega)\exp\left(-\frac{\alpha}{2}z + jd\omega z + \frac{j}{2}\beta_2\omega^2 z\right)\right\} \qquad (4.2)$$

where $\mathcal{F}^{-1}$ is the inverse Fourier transform and U_d is the Fourier spectrum of the data channel.

We begin by investigating the distribution of the power of the data channel, $|u_d|^2$, as a function of length, z. The pulses of the data channel change over the length due to dispersion, self-phase modulation, and attenuation. The length of the fiber is chosen so that we can simulate the dispersive effects and neglect the nonlinear effects. We first simulate without attenuation to emphasize the pulse shape due to spreading. Then attenuation is added. Next we change the group velocity difference. Then we vary the data channel powers.

4.2 Simulation Parameters

The simulation data signal is a $2^{10} - 1$ pseudorandom binary string that is on-off key modulated with optical power of 1 mW with periodic boundary conditions. The fiber has an attenuation of 0.2 dB/km, group velocity dispersion $\beta_2 = -22$ ps^2/km, and Kerr nonlinearity 1.3 W^{-1}km^{-1}. The data channel has a center wavelength of 1530.0413 nm with group velocity difference $d = 1.003$ ps/km relative to the frequency signal. Some of these parameters will vary in the following sections as we study the changes in the

XPM induced phase distortion.

4.3 Without Attenuation

Neglect attenuation for the moment to evaluate the evolution of the data channel due to the material dispersion and how it affects the phase stability.

During propagation, each pulse in the data signal is going to spread outside of its bit window into its neighbors. After some long distance, the energy in each pulse will spread evenly amongst every bit. Therefore, the variance of the data signal's optical power will approach a limit as a function of fiber length. Figure 4.1 shows the data channel power variance over the fiber

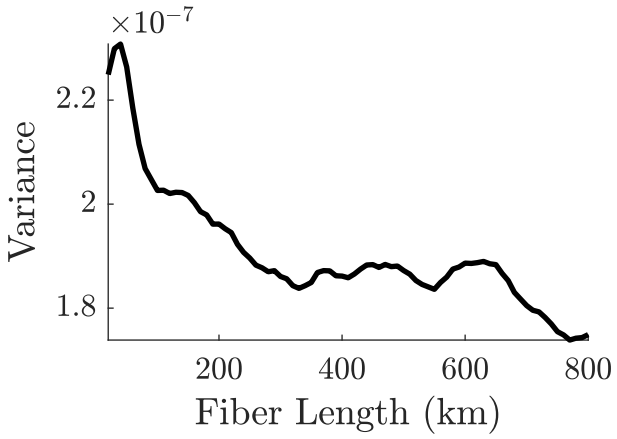

Figure 4.1: Data channel optical power variance vs. fiber length

length of interest, we have not achieved the limit but there is not an appreciable change beyond 800 km. Since the loss is turned off, the mean of the data channel power is fixed, and the range of the variance shows that the data channel power doesn't become significantly larger than the mean.

This is important because the power will be directly related to the amount of cross-talk.

The phase error ϕ clearly grows as a function of distance because at every propagation length the two channels have some cross-talk which keeps accumulating. Figures 4.2a and 4.2b show the mean and variance of the phase distortion due to XPM respectively. The mean of ϕ grows linearly

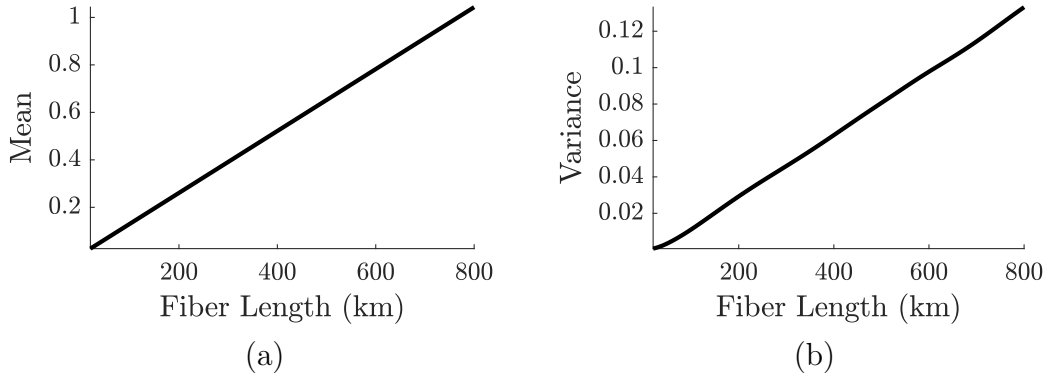

Figure 4.2: (a) Mean of ϕ vs. fiber length (b) Variance of ϕ vs. fiber length

with respect to the fiber length because without a loss mechanism the average energy in the data channel is constant. This signifies a mean additive phase error that can be compensated.

At this point we want to quantify the phase stability using measures from chapter 2. We first consider the first structure equation, $D_{\phi}^{(1)} = \langle[\phi(t+\tau) - \phi(t)]^2\rangle$, which represents the mean phase accumulation. The structure functions are related to the autocorrelation. A typical data transmission will be a collection of random bits that are uncorrelated with eachother. As the data signal propagates through the fiber, every pulse that represents a bit will

spread into its neighbors, thus the amount of time where a bit is correlated with itself increases. Figure 4.3 shows $D_{\phi}^{(1)}$ at different lengths and agrees with this explanation. The phase stabilizes after a short amount of time.

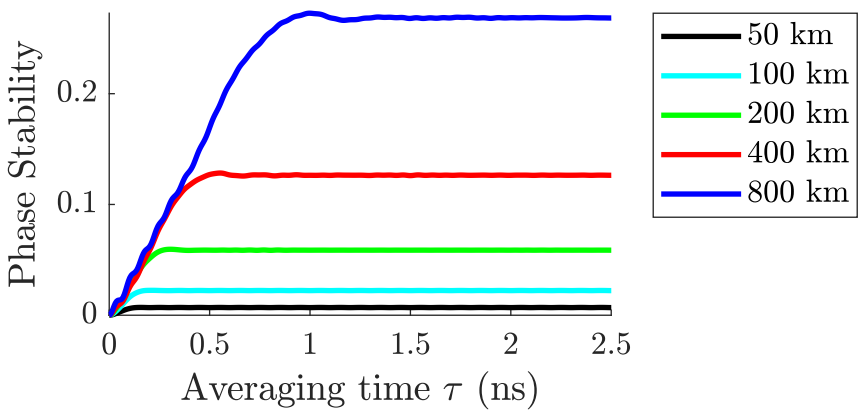

Figure 4.3: Phase Stability vs. averaging time τ

Figure 4.4 shows the Allan Deviation. After a short amount of time, the short term frequency errors are averaged out at the peak, then the Allan Deviation drops off at the rate of τ^{-1}. The Allan Deviation will continue this trend, because there are no long term frequency errors from the XPM. We have compute over a short time interval due to memory limitations, but we can use a linear fit for the τ^{-1} region to determine the Allan Deviation for usual averaging times. At $\tau = 1$ s ADEV $= 3 \times 10^{-15}$, and at $\tau = 10^3$ s ADEV $= 3 \times 10^{-18}$.

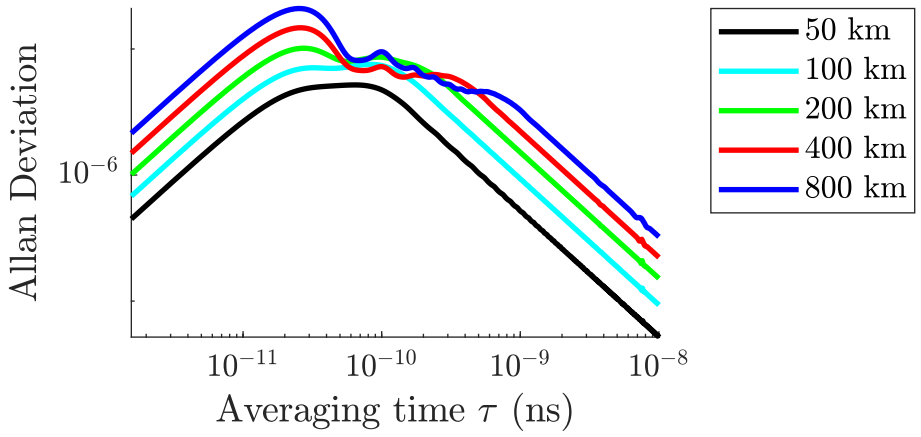

Figure 4.4: Allan Deviation

4.4 With Attenuation

We now add attenuation to the data channel. We expect the results to be bounded above by the phase and frequency stability without attenuation because the effective length before the nonlinearity becomes negligible is 20 km after each amplifier, meaning the cross-talk weakens over a quarter length between amplifiers.

First, we compare the variance of the attenuated data channel with the previous section's. Figure 4.5 shows the data channel's optical power variance. The spikes occur every 80 km corresponding with the amplifiers location, the spikes will grow at distances beyond 800 km because the ASE noise will start accumulating.

The mean and variance of ϕ must also grow over the distance of the fiber, but there are lengths of the fiber which the power is low, so there will be

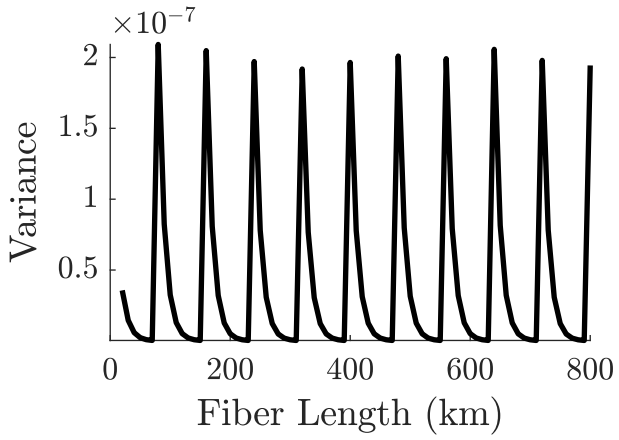

Figure 4.5: Data channel optical power variance vs. fiber length

steps. Figures 4.6a and 4.6 show the mean and variance of ϕ respectively and show the steps where the data channel power is low. The mean and variance are less than those of the previous section.

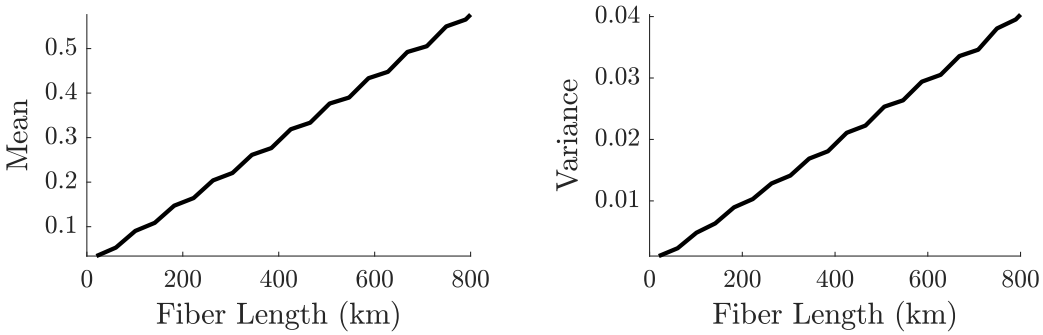

Figure 4.6: (a) Mean of ϕ vs. fiber length (b) Variance of ϕ vs. fiber length

The phase stability computed as the structure function $D_{\phi}^{(1)}$ will asymptote like in the previous section. Since this depends on the pulse spreading due to dispersion, the asymptotes occur at the same times. However, the

phase stability will be less due to attenuation. Figure 4.7 shows $D_{\phi}^{(1)}$ for different fiber lengths and agrees with the previous explanation.

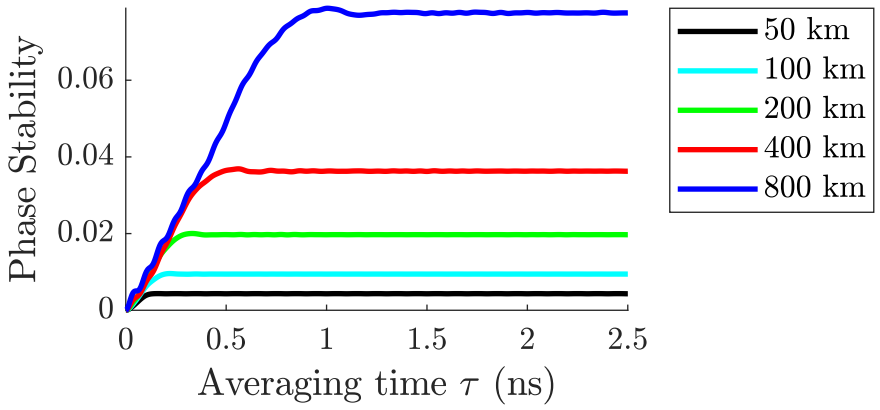

Figure 4.7: Phase stability with attenuation

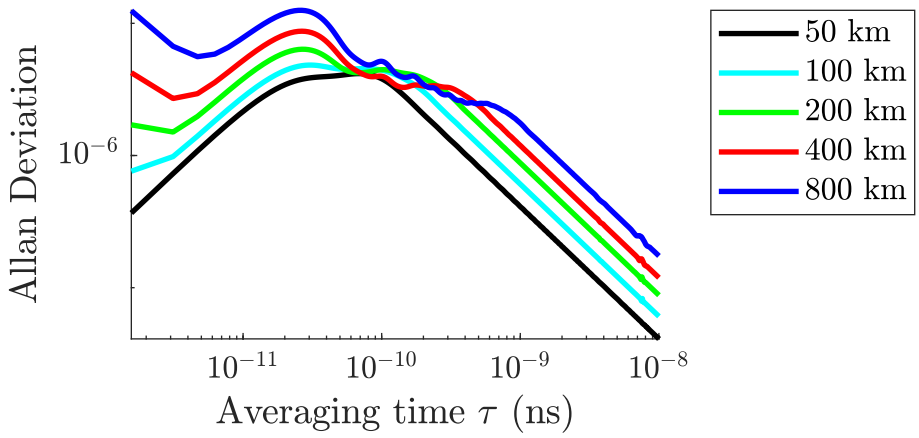

Figure 4.8: Allan Deviation with attenuation

Finally, the Allan Deviation will be comparable to the results in the previous section. Figure 4.8 shows the Allan Deviation for several fiber lengths, the bump at the early time intervals corresponds with larger short term fre-

quency errors, but they are averaged out very quickly and, once again, there are no long term frequency errors. The Allan Deviation will continue at a rate of τ^{-1}. At $\tau = 1$ s ADEV $= 10^{-15}$, and at $\tau = 10^3$ s ADEV $= 10^{-18}$.

4.5 Varying the Group Velocity Difference

The relative group velocity difference governs the rate that a bit pulse will travel through a fixed time point. The group velocity difference is related to the separation between the center frequencies of the data and frequency channel. The value $d = 1.003$ ps/km was chosen because it corresponds with the greatest group velocity difference while adhering to the ITU grid standard. As the distance between the center frequencies decreases, the group velocity difference increases. Figure 4.9 shows the phase stability for different group velocity differences.

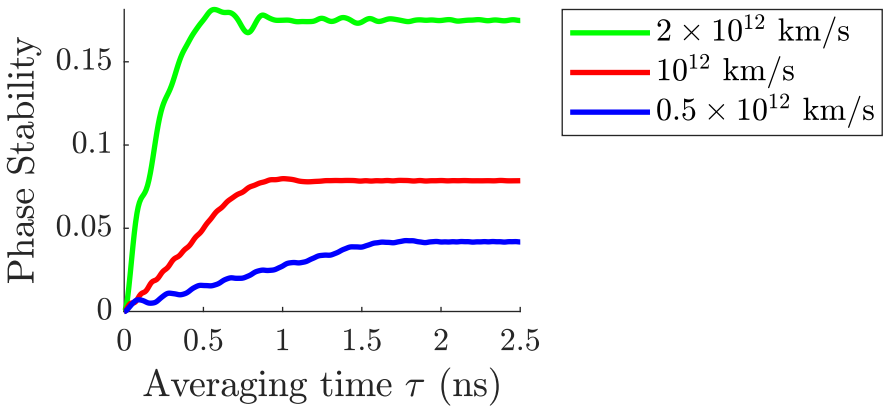

Figure 4.9: Phase stability vs. group velocity difference

4.6 Chapter Remarks

Since the bits of any data channel are uncorrelated, the phase stability will asymptote at an averaging time corresponding to the duration of a bit window and the relative group velocity of the data channel. When the relative group velocity is greater, the asymptote occurs sooner because the data channel passes through a fixed time point at a much greater rate.

The Allan Deviation represents the amount of frequency error. Experiments performing frequency transfer with a frequency signal and data channel located on the ITU standards have Allan Deviation values comparable to our simulated values [4] [2]. The source of error in the experiments is due to temperature. So we see that moving the frequency signal in the interstices of two data channels gives a frequency error on the order of environmental effects.

Chapter 5: Conclusion

A frequency signal in an optical fiber suffers optical impairments due to the medium. By placing requirements on the location and optical power of the frequency signal, we can eliminate a majority of the impairments.

Systems performing frequency transfer over optical fiber place the frequency signal at a center frequency designated for a data channel which wastes a significant amount of bandwidth. We can solve this issue by moving the frequency signal into the interstices of the data channels. However, placing the frequency signal closer to the data channels will increase the amount of cross-talk which causes an increased amount of phase and frequency error.

We computed the amount of frequency error due to cross-talk using the Allan Deviation and found that it was comparable to environmental effects in experimental setups. This means it is feasible to move the frequency signal to the interstices of two data channels without significant error due to cross-phase modulation.

5.1 Future Work

The length of the optical fiber was chosen to eliminate the effects of self-phase modulation on the data channel. Increasing the length of the transmission to 3000–4000 km, comparable to the length of research institutions in the United States, requires computing the effects of the self-phase modulation. This was avoided in our work because the amount of time necessary to solve the Nonlinear Schrödinger Equation using the split-step Fourier method was prohibitively long.

Bibliography

[1] D. Allan and M. Weiss, "Accurate Time and Frequency Transfer During Common-View of a GPS Satellite," *34th Annual Symposium on Frequency Control*, no. May, pp. 334–346, 1980.

[2] E. Cantin, N. Quintin, F. Wiotte, C. Chardonnet, A. Amy-Klein, and O. Lopez, "Progress on the REFIMEVE+ project for optical frequency standard dissemination," in *Frequency and Time Forum and IEEE International Frequency Control Symposium (EFTF/IFC), 2017 Joint Conference of the European*, pp. 378–380, IEEE, 2017.

[3] K. Turza, A. Binczewski, and W. Bogacki, "Time and frequency transfer in modern DWDM telecommunication networks," pp. 368–370, 2017.

[4] J. Serrano, M. Lipinski, T. Wlostowski, E. Gousiou, E. van der Bij, and M. Cattin, "The White Rabbit project," in *2nd International Beam Instrumentation Conference*, p. THBL2, 2013.

[5] P. Krehlik, L. Sliwczynski, J. Dostal, J. Radil, V. Smotlacha, and R. Velc, "CLONETS - Clock network services: Strategy and innovation for clock services over optical-fibre networks," *International Conference on Transparent Optical Networks*, vol. Part F81-E, no. 2008, pp. 1–2, 2017.

[6] G. P. Agrawal, *Fiber-Optic Communication Systems*. Wiley Series in Microwave and Optical Engineering, Wiley, 2012.

[7] G. P. Agrawal, *Nonlinear fiber optics*. Academic Press, 2013.

[8] ITU-T, "G.694.1 (02/2012), Spectral grids for WDM applications: DWDM frequency grid," *Series G.694.1*, pp. 1–16, 2012.

[9] J. G. Proakis, *Digital Communications*. Electrical engineering series, McGraw-Hill, 2001.

[10] D. B. Leeson, "Oscillator phase noise: A 50-year review," *IEEE Transactions on Ultrasonics, Ferroelectrics, and Frequency Control*, vol. 63, no. 8, pp. 1208–1225, 2016.

[11] D. W. Allan, N. Ashby, and C. C. Hodge, "The science of timekeeping," *Hewlett Packard application note 1289*, pp. 1–88, 1997.

[12] B. E. Blair, *Time and Frequency: Theory and Fundamentals*. No. no. 140 in Monograph, U.S. National Bureau of Standards, 1974.

[13] Ł. Śliwczyński, P. Krehlik, and M. Lipiński, "Optical fibers in time and frequency transfer," *Measurement Science and Technology*, vol. 21, no. 7, p. 75302, 2010.

[14] Ł. Śliwczyński and P. Krehlik, "Multipoint joint time and frequency dissemination in delay-stabilized fiber optic links," *IEEE Transactions on Ultrasonics, Ferroelectrics, and Frequency Control*, vol. 62, no. 3, pp. 412–420, 2015.

[15] D. W. Allan, J. H. Shoaf, and D. Halford, "Statistics of Time and Frequency Data Analysis," in *Time and Frequency: Theory and Fundamentals* (B. E. Blair, ed.), p. 151, 1974.

[16] J. Rutman, "Oscillator Specifications: A Review of Classical and New Ideas," *31st Annual Symposium on Frequency Control. 1977*, pp. 291–301, 1977.

[17] W. J. Riley, *Handbook of Frequency Stability Analysis*, vol. 31. 1994.

[18] R. B. Blackman and J. W. Tukey, "the Measurement of Power Spectra From the Point of View of Communications Engineering," 1958.

[19] W. C. Lindsey, "Theory of Oscillator Instability Based Upon Structure Functions," *Proceedings of the IEEE*, vol. 64, no. 12, pp. 1652–1666, 1976.

[20] E. O. Schulz-DuBois and I. Rehberg, "Structure function in lieu of correlation function," *Applied Physics*, vol. 24, no. 4, pp. 323–329, 1981.

[21] P. Kartaschoff, *Frequency and Time*. New York: Academic Press, 1978.

[22] C. R. Menyuk, "Transmission of a frequency channel through a long-haul optical fiber communications link," in *2015 Joint Conference of the IEEE International Frequency Control Symposium the European Frequency and Time Forum*, pp. 736–741, April 2015.